Improvement of Output Voltage with SVM in Three-phase AC to DC Isolated Matrix Converter

Goh Teck Chiang
Nagaoka University of Technology
Nagaoka, Japan
tcgoh@vos.nagaokaut.ac.jp

Koji Orikawa
Nagaoka University of Technology
Nagaoka, Japan
orikawa@vos.nagaokaut.ac.jp

Yoshiya Ohnuma
Nagaoka University of Technology
Nagaoka, Japan
ohnuma@stn.nagaokaut.ac.jp

Jun-ichi Itoh
Nagaoka University of Technology
Nagaoka, Japan
itoh@vos.nagaokaut.ac.jp

***Abstract*—This paper discusses and evaluates the performance of a 50-kVA three-phase AC to DC matrix converter. Comparing to the conventional converter, which consists of a PWM rectifier and an inverter, the matrix converter does not require a large reactor at the three-phase input side, and require no DC smoothing capacitor at the DC link part. A space vector modulation based on the virtual AC-DC-AC conversion with four-step commutation patterns is proposed for the converter. From the experimental results, the converter can obtain 2.49% THD on the input current and achieves approximately 91.4% efficiency at 40kW.**

Keywords—Matrix converter; three-phase to single phase; AC-DC; Space vector modulation

I. INTRODUCTION

Three-phase AC-DC power converters have received significant attentions in community. In particular, heavy industrials apply these converters in order to supply sufficient DC power to specific equipment, such as the communication equipment, from a three-phase AC power grid or generators. In these applications, for the protection purpose and noise elimination, an isolated transformer is typically being used in the converter. However, the isolated transformer that generally connects to the power grid is consuming large amount of space.

Figure 1 shows the conventional AC-DC converter which is typically applied in the spoken applications [1-2]. In order to isolate the converter from the grid supply, a large transformer is generally connected between the grid and the AC-DC converter. Then, the structure of AC-DC converter is composed from a three-phase diode bridge rectifier and a buck converter. However, the diode bridge rectifier has poor harmonic components in the input current and also the electrolytic capacitors are required at the rear end of the rectifier to reduce the DC ripple waveforms. On the other hand, the buck converter is used to regulate the DC output voltage that meets the application requirements. In a high power system, the size of the transformer is generally large to ensure that current density is sufficient, which becomes a significant drawback for this converter.

In order to reduce the size of the transformer and also to improve the harmonic components, Figure 2 shows a better option of the AC-DC converter. The circuit consists of a PWM rectifier and a high frequency resonant converter with a small size isolation transformer [3-4]. The PWM rectifier is employed in order to improve the harmonic components of the input current. Then, high switching frequency resonant converter is employed in order to reduce the size of the transformer. Even the harmonic component issue in the input current can be greatly improved; the drawback is a sufficient value of reactor is required at the front end of the PWM rectifier.

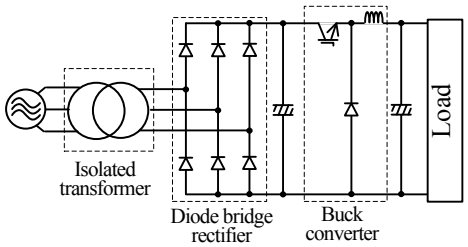

Fig. 1. AC-DC converter with diode bridge rectifier and buck converter.

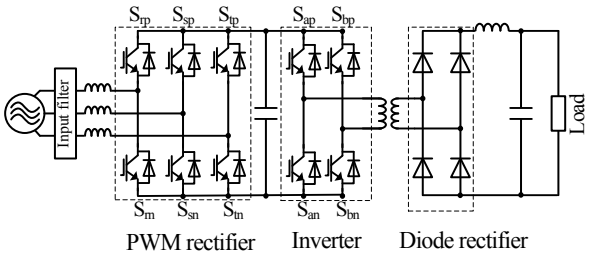

Fig. 2. AC-DC converter with PWM rectifier and inverter.

Moreover, this converter produces higher losses due to the switching intervals in the PWM rectifier. Similar to the previous converter, a smoothing DC capacitor is required to connect between the PWM rectifier and a half bridge converter in order to reduce the DC ripple components. On the other hand, the full bridge converter which is connected to the isolated transformer, is employed with a high switching frequency and eventually produces a large amount of switching losses. Then, the rear end of the converter is connected to the full bridge diode rectifier in order to transform the AC voltage into the DC voltage.

In this paper, the authors discuss an AC-DC direct conversion circuit based on the concept of matrix converter with a space vector modulation (SVM) [5-6]. The matrix

converter is possible to directly convert three-phase AC waveforms into three-phase AC waveforms and enables a controllable frequency and output voltage amplitude, which requires no passive components at the DC bus. In this paper, the matrix converter is composed from 12 unit of switching devices only because of the three phase input single output structure, as shown in Fig. 3. Comparing to the conventional circuit, the matrix converter can achieve two stages conversion and improve the efficiency. Furthermore, the matrix converter can control the input current and output current at one time to ensure low harmonic components of sinusoidal waveforms can be achieved. On the other hand, a small size isolated transformer can be used because the high switching frequency is possible.

The high frequency link isolation matrix converter with resonance converter has been discussed [7]. In Ref. [7], the authors discussed a safe commutation in the matrix converter during the zero voltage switching (ZVS) operation. In order to achieve ZVS, additional switches are employed in the diode rectifier so that the diode rectifier can become a structure of resonance converter. Furthermore, additional inductor and capacitor are included at the output of matrix converter to ensure ZVS is achieved at low current. However, the control to achieve ZVS becomes complicated, thus, not all the switching period can achieve ZVS operation which result the efficiency is dropping.

In this paper, a simple matrix converter structure as shown in Fig. 3 is implemented with SVM to reduce the number of the switching. Also, a 4-step commutation method is included to compensate the pulse error during the switching intervals. The proposed control enables low THD components on input current and also achieves high efficiency. First of all, the circuit structure is explained in the second chapter. Then, the control strategies are illustrated and detailed in the chapter 3. In particular, the beneficial of SVM with the 4-step commutation is shown to improve the output voltage error during the switching intervals. Simulation and experimental results are provided in the late chapters to demonstrate the circuit performance. Finally, the validity of the proposed method is evaluated in subjects to the harmonic components and efficiency.

II. CIRCUIT TOPOLOGY

Figure 3 shows the circuit structure of the matrix converter. A small LC filter is employed at the front end of the converter to reduce switching ripples. Then, a three-phase AC to single phase AC matrix converter is employed between the grid supply and the isolated transformer. The isolated transformer is designed based on a general-purpose method. Each of the switching modules in the matrix converter is composed from a two anti-series connected IGBT, where 6 modules are employed in the matrix converter. Then, the secondary side of the transformer is devoted by a standard diode bridge rectifier to obtain DC waveform. As shown in the Fig. 3, the 50-Hz grid voltage is directly converted to the input voltage of the transformer by the matrix converter without any passive components.

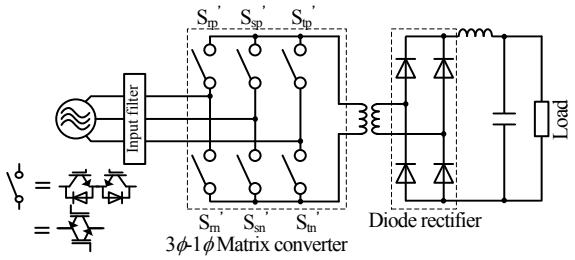

Fig. 3. Circuit strucutre with matrix converter.

The size and weight of the AC-DC isolated matrix converter can be greatly reduced because the passive components that are used in the conventional converter (as shown in Fig.2); the boost-up reactor in the front end and the smoothing capacitor at the DC bus, are not required.

Furthermore, due to the reason of the high switching frequency is possible in the matrix converter, the size of the isolated transformer can be reduced, comparing to the commercial frequency isolated transformer.

However, the converter has two issues in the control that needs to be addressed. Due to direct conversion, the input current and output current are required to control simultaneously, which results the control technique becomes complicated. Furthermore, commutation patterns are required in the switching intervals to ensure switching errors are not occurring. To simplify the complexity of the control strategies, a virtual AC-DC-AC conversion technique is proposed.

III. PROPOSED CONTROL STRATEGIES

This chapter discusses the control techniques of the matrix converter. In order to simplify the control techniques, a virtual AC-DC-AC conversion technique which has been discussed in Ref [8] is referred.

In Figs. 2 and 3, the input voltage is represented as ${}^t[v_r,v_s,v_t]$ and the output voltage (transformer input voltage) is represented as ${}^t[v_a,v_b]$. S_{xy} represents the switching function of the switches, when S_{xy} is turned on, S_{xy}=1 and when S_{xy} is turned off, S_{xy}=0. The switching intervals for Fig. 2 can be expressed as (1), where the left block is the full bridge inverter (S_{ap}, S_{an}, S_{bp}, S_{bn}) and the right block is the PWM rectifier (S_{rp}, S_{sp}, S_{tp}, S_{rn}, S_{sn}, S_{tn}).

$$\begin{bmatrix} v_a \\ v_b \end{bmatrix} = \begin{bmatrix} s_{ap} & s_{an} \\ s_{bp} & s_{bn} \end{bmatrix} \begin{bmatrix} s_{rp} & s_{sp} & s_{tp} \\ s_{rn} & s_{sn} & s_{tn} \end{bmatrix} \begin{bmatrix} v_r \\ v_s \\ v_t \end{bmatrix}. \quad (1)$$

$$\begin{bmatrix} v_a \\ v_b \end{bmatrix} = \begin{bmatrix} s_{rp}' & s_{sp}' & s_{tp}' \\ s_{rn}' & s_{sn}' & s_{tn}' \end{bmatrix} \begin{bmatrix} v_r \\ v_s \\ v_t \end{bmatrix}. \quad (2)$$

$$\begin{bmatrix} s_{rp}' & s_{sp}' & s_{tp}' \\ s_{rn}' & s_{sn}' & s_{tn}' \end{bmatrix} = \begin{bmatrix} s_{ap} & s_{an} \\ s_{bp} & s_{bn} \end{bmatrix} \begin{bmatrix} s_{rp} & s_{sp} & s_{tp} \\ s_{rn} & s_{sn} & s_{tn} \end{bmatrix}. \quad (3)$$

In the matrix converter, the relationship between the output voltage ${}^t[v_a,v_b]$ and input voltage ${}^t[v_r,v_s,v_t]$ can be expressed in (2), where S_{xy}' represents the switching intervals for the matrix

converter. Based on (1), the switching units in (2) can be expressed into (3), that is, the switching units are the multiplication between the left block and the right block.

Figure 4 shows the control block diagram. Here, a PI regulator is used in order to regulate the input current command i^* and the output current i_{out}. Then, the input current commands are derived from the input voltages which are transformed from a three-phase voltage into a two dimensional vector in the stationary reference frame. The input current command i^* is taken into account in order to calculate the rotation angle of the input current angles to ensure unity input power factor, and also, it is used to determine the amplitude of the input current.

Figure 5 illustrates the input current command i^* in the voltage vector diagram which is based on the space vector modulation. According to the position of i^*, then the corresponding voltage vector will be selected. (For example, in Fig. 5, the input current command i^* is located in the area where V_1 and V_2 will be selected.) Then, the α and β fundamental components of the input current commands are derived into voltage components V_α and V_β. In subjects to the duty periods, T_1, T_2 and zero vectors T_z, the voltage vectors that are responding to the fundamental voltage components can be derived into V_{1a}, V_{1b}, V_{2a} and V_{2b}, which can be expressed in (4).

$$
\begin{aligned}
T_1 &= \frac{1}{|A|}\begin{vmatrix} v_\alpha & v_{2\alpha} \\ v_\beta & v_{2\beta} \end{vmatrix}. \\
T_2 &= \frac{1}{|A|}\begin{vmatrix} v_{1\alpha} & v_\alpha \\ v_{1\beta} & v_\beta \end{vmatrix}. \\
T_z &= 1-(T_1+T_2). \\
|A| &= \begin{vmatrix} v_{1\alpha} & v_{2\alpha} \\ v_{1\beta} & v_{2\beta} \end{vmatrix}.
\end{aligned}
\tag{4}
$$

From (4), switching patterns can be formed in according to the desired voltage vectors and duty periods. However, the output voltage of the matrix converter is a square waveform that has voltage polarity which can be expressed in (5). Note that, the switching duty is considered as 50% which is the same as in the conventional full bridge converter.

$$
\begin{bmatrix} s_{ap} & s_{an} \\ s_{bp} & s_{bn} \end{bmatrix} = \left\{ \begin{bmatrix} 1 & 0 \\ 0 & 1 \end{bmatrix}, \begin{bmatrix} 0 & 1 \\ 1 & 0 \end{bmatrix} \right\}. \tag{5}
$$

Therefore, when (5) is substituted into (3), two patterns of switching intervals are happening in the virtual PWM inverter. When the virtual PWM inverter is equaled ^{t}[1 0 0 1], no particular changes are required. However, when the virtual PWM inverter becomes ^{t}[0 1 1 0], an inverse form of switching intervals are required.

SVM shows the advantages in considering the complicated switching intervals which is subjected to the condition of (5), because SVM provides flexibility in determining the duty period. Table 1 shows the complete switching table for the

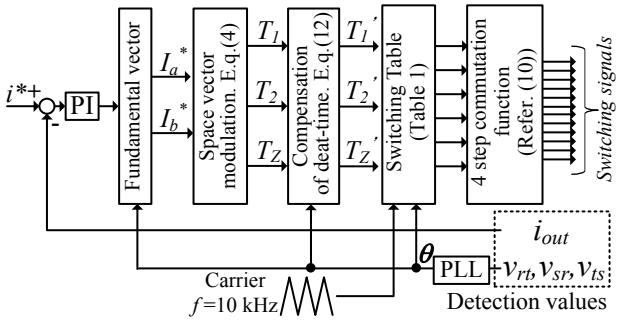

Fig. 4. Control block diagram.

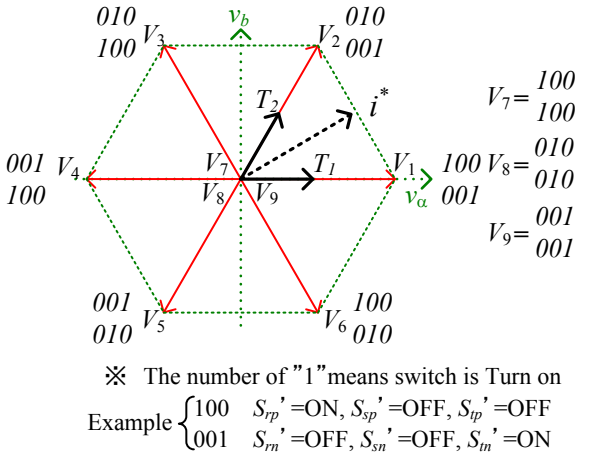

Fig. 5. Fundamental voltage vector.

TABLE I. SWITCHING TABLE FOR THE MATRIX CONVERTER

		Area1	Area2	Area3	Area4	Area5	Area6
Positive	State1	$V_1=\begin{smallmatrix}100\\001\end{smallmatrix}$	$V_2=\begin{smallmatrix}010\\001\end{smallmatrix}$	$V_3=\begin{smallmatrix}010\\100\end{smallmatrix}$	$V_4=\begin{smallmatrix}001\\100\end{smallmatrix}$	$V_5=\begin{smallmatrix}001\\010\end{smallmatrix}$	$V_6=\begin{smallmatrix}100\\010\end{smallmatrix}$
	State2	$V_2=\begin{smallmatrix}010\\001\end{smallmatrix}$	$V_3=\begin{smallmatrix}010\\100\end{smallmatrix}$	$V_4=\begin{smallmatrix}001\\100\end{smallmatrix}$	$V_5=\begin{smallmatrix}001\\010\end{smallmatrix}$	$V_6=\begin{smallmatrix}100\\010\end{smallmatrix}$	$V_1=\begin{smallmatrix}100\\001\end{smallmatrix}$
	State3	$V_8=\begin{smallmatrix}010\\010\end{smallmatrix}$	$V_7=\begin{smallmatrix}100\\100\end{smallmatrix}$	$V_9=\begin{smallmatrix}001\\001\end{smallmatrix}$	$V_8=\begin{smallmatrix}010\\010\end{smallmatrix}$	$V_7=\begin{smallmatrix}100\\100\end{smallmatrix}$	$V_9=\begin{smallmatrix}001\\001\end{smallmatrix}$
Negative	State4	$V_5=\begin{smallmatrix}001\\010\end{smallmatrix}$	$V_6=\begin{smallmatrix}100\\010\end{smallmatrix}$	$V_1=\begin{smallmatrix}100\\001\end{smallmatrix}$	$V_2=\begin{smallmatrix}010\\001\end{smallmatrix}$	$V_3=\begin{smallmatrix}010\\100\end{smallmatrix}$	$V_4=\begin{smallmatrix}001\\100\end{smallmatrix}$
	State5	$V_4=\begin{smallmatrix}001\\100\end{smallmatrix}$	$V_5=\begin{smallmatrix}001\\010\end{smallmatrix}$	$V_6=\begin{smallmatrix}100\\010\end{smallmatrix}$	$V_1=\begin{smallmatrix}100\\001\end{smallmatrix}$	$V_2=\begin{smallmatrix}010\\001\end{smallmatrix}$	$V_3=\begin{smallmatrix}010\\100\end{smallmatrix}$
	State6	$V_7=\begin{smallmatrix}100\\100\end{smallmatrix}$	$V_9=\begin{smallmatrix}001\\001\end{smallmatrix}$	$V_8=\begin{smallmatrix}010\\010\end{smallmatrix}$	$V_7=\begin{smallmatrix}100\\100\end{smallmatrix}$	$V_9=\begin{smallmatrix}001\\001\end{smallmatrix}$	$V_8=\begin{smallmatrix}010\\010\end{smallmatrix}$

matrix converter based on the SVM. Positive and negative show the polarity of the output voltage. States 1, 2 and 3 represent the T_1, T$_2$ and T_z for positive voltage and states 4, 5 and 6 represent the T_1, T_2 and T_z for negative voltage. In order to output both positive and negative polarity of voltages in one switching period, 6 kinds of voltage vector are required. From Table 1, in each area for each of the state, upper switches are represented as S_{rp}', S_{sp}', and S_{tp}' and lower switches are represented as S_{rn}', S_{sn}'and S_{tn}'.

Due to the reason of direct conversion, in order to avoid short circuit in term of voltage and open circuits in term of

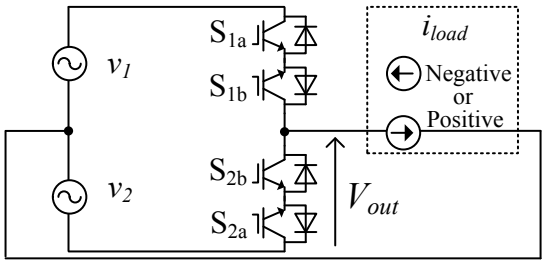

Fig. 8. Commutation model.

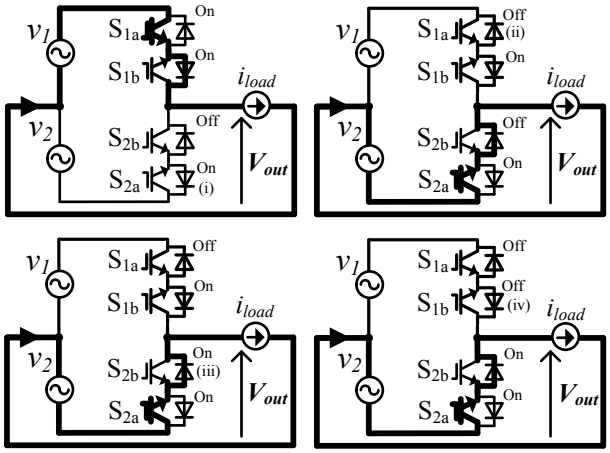

(a) Current is positive.

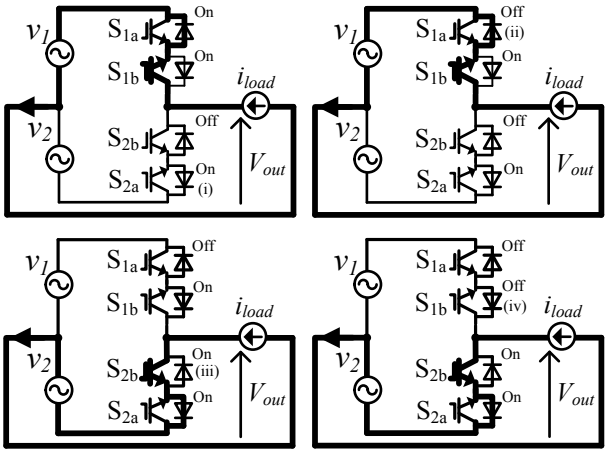

(b) Current is negative.

Fig. 9. Sequence of the 4-step commutation.

current, a continuous 4-step commutation pattern is required in each switching intervals. In the matrix converter, the commutation is decided by input absolute voltage (the relationship between maximum, medium and minimum phase).

Figure 6 shows a simplify model of the matrix converter to demonstrate the 4-step commutation patterns. Note that since the output voltage is formed directly depending on the input voltage, v_1 and v_2 represent the input voltage which can be the maximum voltage, medium voltage or the minimum voltage. The 4-step commutation is based on a voltage-dependent

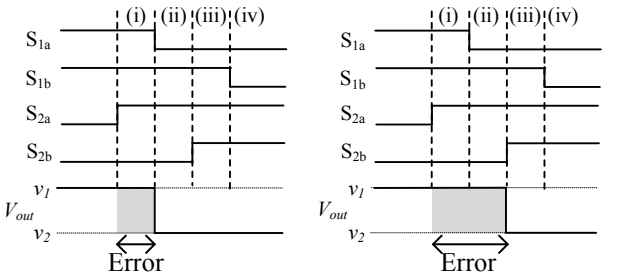

(a) Current direction from positive to to negative.

(b) Current direction from negative to positive.

Fig. 6. Detail of commutation patterns.

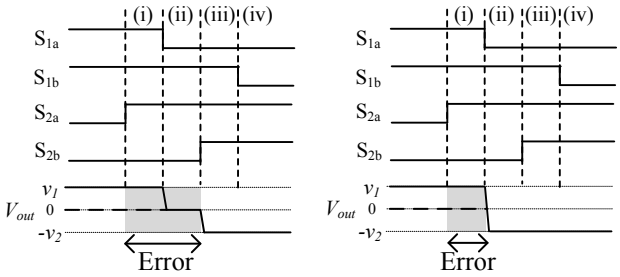

(a) Current direction from positive to to negative.

(b) Current direction from negative to positive.

Fig. 7. During the commutation sequence.

commutation in a classical matrix converter [9]. In the voltage-dependent commutation, output voltage errors occur subsequently depending on the current direction. Figures 7(a) and (b) show the sequence of the 4-step commutation when the output current is positive and negative, respectively. Note that the switching intervals in Fig. 7 demonstrate the switching when S_{2a} and S_{2b} are turning on and S_{1a} and S_{1b} are turning off. In Fig. 7(a), even the S_{2a} is turned off at the first step, the flow of the output current remains at the same pathway. Then, the output current changes the pathway (flow into S_{2a} and S_{2b}) at the second step of the commutation pattern. In Fig. 7(b), in the events of first and second steps, the output current remains at the same pathway. Then, the output current changes the pathway at the third step of the commutation pattern.

Figures 8(a) and (b) summarizes that, under the same sequence in commutation, when $V_1 > V_2$, there is one delay occurring in the output voltage when the current direction is positive, and however, there are two delays occurring in the output voltage when then current direction is negative. Furthermore, in the matrix converter, the current direction might change during the commutation sequence as shown in Figs. 9(a) and (b).

In Fig. 8 (a), when the current is positive, the polarity of the output voltage is changed in the step 2 during commutation, there are two delays occurring in the output voltage. In Fig. 8(b), when the current is negative, in the case of Fig. 7(b), two delays occurring in the output voltage but when the polarity of the output voltage changes during the commutation sequence, only one delay occurring in the output voltage.

As a result, the voltage error which is caused by the commutation needs to be compensated. In order to compensate the voltage error, one period of dead time is added into the duty cycle as expressed in (6). The dead time period is added to balance the output voltage in each switching periods. Figure 10 illustrates the error occurring in the output voltage error due to the commutation.

$$\begin{cases} T_1^{'} = T_1 \\ T_2^{'} = T_2 + T_d \\ T_Z^{'} = 1-(T_1^{'}+T_2^{'}), \\ (T_1 > T_2) \end{cases} \quad \begin{cases} T_1^{'} = T_1 + T_d \\ T_2^{'} = T_2 \\ T_Z^{'} = 1-(T_1^{'}+T_2^{'}), \\ (T_1 < T_2) \end{cases} \tag{6}$$

IV. Simulation Results

The simulation parameters are follows, the input voltage is 200 V, the input frequency is 50 Hz, the switching frequency is 10 kHz, cut-off frequency of LC filter is 1 kHz and the transformer ratio is 1:2.6. Note that the simulation is running in a RL load condition without the 4-step commutation. Furthermore, a current step control is included in the result to demonstrate that the matrix converter can response effectively to a load change.

Figure 11 shows simulation results without the 4-step commutation. In Fig. 11, from the sinusoidal input voltage and current waveforms, unity power factor is achieved. The DC output voltage is 400 V, and the current step control is applied on 72 ms. Note that the input current can response to the load current effectively when the current step control is implemented. Moreover, there is no fluctuation of the DC output voltage. Figure 12 demonstrates an extended image of the Fig. 11 during the transient period. A smooth transition can be noticed in the output DC current. The 10-kHz square wave transformer voltage is achieved even the input waveform is a 50-Hz voltage. Furthermore, no significant spike voltage occurring in the transformer voltage and DC output voltage.

V. Experimental Evaluations

Table 2 shows the experimental parameters. Figure 13 shows the experimental results at 50 kW condition. From the results, input voltage and current waveforms show that unity power factor is achieved. The DC output voltage is 400 V and the DC output current is 125 A.

Figure 14 demonstrates the input power factor and efficiency that are subjected to the output power. From the results, it is confirmed that the input power factor achieves

TABLE II. Experimental Parameters

Items	Value	Items		Value
Input voltage	100 V	PI controller	K_p	0.8 p.u.
Input frequency	50 Hz		T_i	0.7 μs
Output frequency	30 Hz	Commutation time		3 μs
Output R-load	1~20 Ω	Input filter	L	0.75 mH
Output L-load	1 mH		C	15.4 μF
Carrier frequency	10 kHz		Cut-off frequency	1.5 kHz

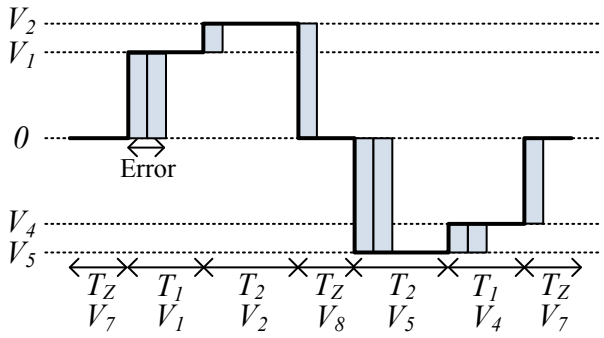

Fig. 10. Output voltage error due to the commutation.

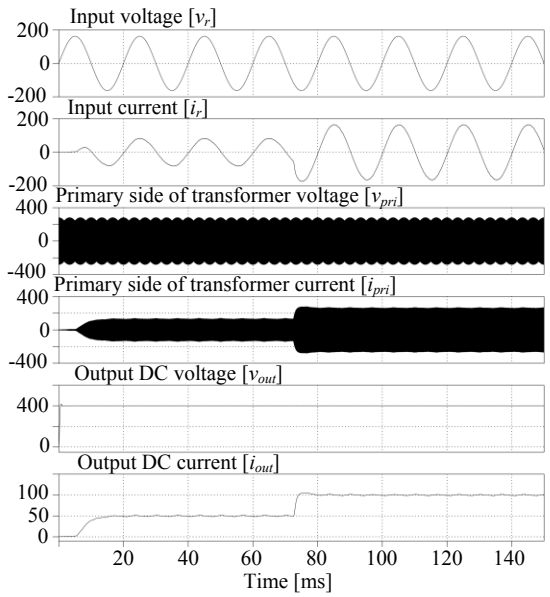

Fig. 11. Simulation results (without 4-step commutation).

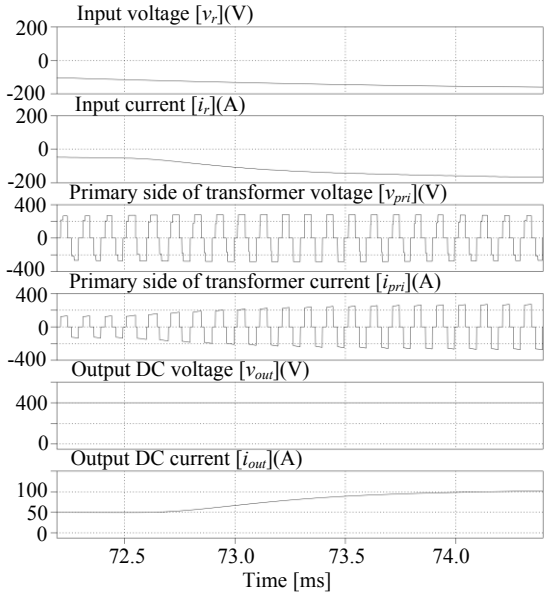

Fig. 12. Extended results during the transition period.

99%. Also, the matrix converter can achieve efficiency 91.4%. Note that the efficiency can be further improved by employing the reverse-blocking IGBT in the matrix converter.

Figure 15 shows the difference between two results, where in Fig. 15(a) the voltage error compensation is not included and in Fig. 15(b) the voltage error compensation is included. From Fig. 15(a) it can be noticed that the DC output current contains frequency components due to the imbalance output voltage. Fig. 15(b) demonstrates that the frequency components can be suppressed after implementing the voltage error compensation. Furthermore, the input current THD can be improved from 4.15% to 2.49% at 40 kW.

VI. CONCLUSION

This paper discussed and evaluated a direct type of energy conversion three-phase AC-DC converter. The matrix converter can achieve unity power factor and high efficiency. Moreover, the converter is small in size because (i) no passive components are required such as the boost reactors and electrolytic capacitors, and (ii) high frequency isolated transformer can be used. The authors utilize the simplicity of a virtual AC-DC-AC concept and propose a SVM control techniques. Furthermore, a compensation method for the output voltage, where the output voltage error is caused by the 4-step commutation pattern, is considered and proposed. From the simulation and experimental results, the matrix converter shows that it can achieve 99% unity power factor and 91.4 % efficiency at a 50 kW condition. Moreover, the matrix converter also enables low harmonic components in the input current; the experimental results shows that the input current THD is 2.49 % at a 40 kW condition.

REFERENCES

[1] Salmon, J.C. "Operating a three-phase diode rectifier with a low-input current distortion using a series-connected dual boost converter", *IEEE Trans. on Power Electronics*, Vol. 11, Issue. 4, pp.592-603, Jul 1996

[2] Hengchun Mao, Lee, F. C. Y., Boroyevich, D. and Hiti, S., "Review of high-performance three phase power-factor correction circuits", *IEEE Trans. on Industrial Electronics*, Vol. 44, Issue. 4, pp. 437-446, Aug 1997

[3] Kikuchi, J. and Lipo, T.A. "Three-phase PWM boost-buck rectifiers with power- regenerating capability", *IEEE Trans. on Industry Applications*, Vol. 38, Issue. 5, pp. 1361-1369, Sep/Oct 2002

[4] Zhonghui Bing, Xiong Du and Jian Sun, "Control of Three-phase PWM Rectifiers using a single DC current sensor", *IEEE Trans. on Power Electronics*, Vol. 26, Issue. 6, pp. 1800-1808-, June 2011

[5] Wheeler, P.W, Rodriguez, J., Clare, J.C., Empringham, L., and Weinstein, A. "Matrix Converters: a technology review", *IEEE Trans. on Industrial Electronics*, Vol. 49, Issue. 2, pp. 276-288, 2002

[6] Miura, Y., Kokubo, S., Maekawa, D., Horie, S., Ise, T., Momose, T. and Sato, Y. "Power modulation control of three-phase to single-phase matrix converter for a gas engine cogeneration system", IEEE PESC, pp. 2704- 2710

[7] Garcia-Gil, R.; Espi, J.M., Dede, E.J.; and Sanchis-Kilders, E. "A bidirectional and isolated three-phase rectifier with soft-switching operation", *IEEE Trans. on Industrial Electronics*, Vol. 52, Issue. 3, pp. 765-773, June 2005

[8] Goh Teck Chiang and Itoh, J. –I. "DC/DC Boost Converter Functionality in a Three-Phase Indirect Matrix Converter", *IEEE Trans. on Power Electronics*, Vol. 26, Issue. 5, pp. 1599-1607, May 2011

[9] K. Kato, J. Itoh: "A Novel Control Method for Direct Interface Converters used for DC and AC Power Supplies", EPE, pp. 1-10 (2007)

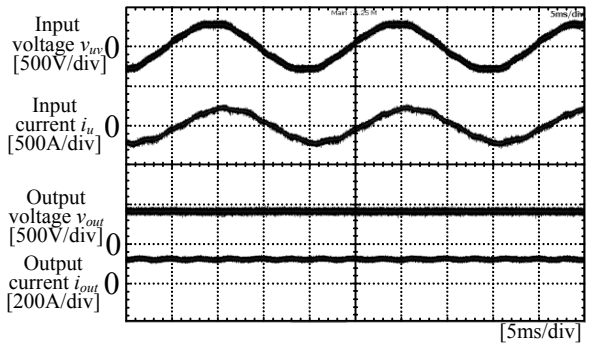

Fig. 13. Experimental waveforms at 50kW condition.

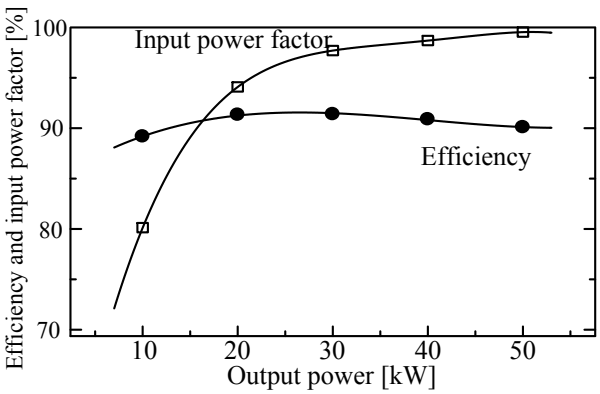

Fig. 14. Efficiency and power factor.

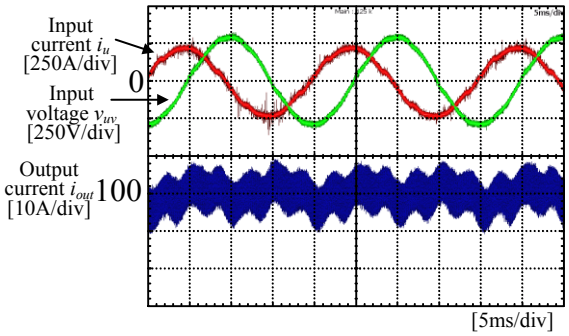

(a) Without the voltage error compensation.

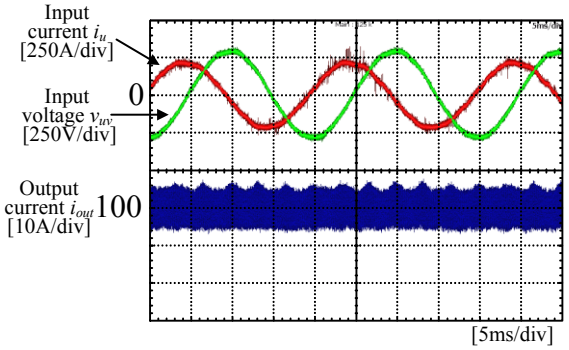

(b) With the voltage error compensation

Fig. 15. Experimental results of the output current.